

Phosphonium Ionic Liquid as Interfacial Agent of Layered Double Hydroxide: Application to a pectin matrix

Luanda Lins¹, Valeria Bugatti², Sébastien Livi^{1*} and Giuliana Gorrasi^{2*}

¹Université de Lyon, F-69003, Lyon, France; INSA Lyon, F-69621, Villeurbanne, France CNRS, UMR 5223, Ingénierie des Matériaux Polymères.

²Department of Industrial Engineering -University of Salerno-via Giovanni Paolo II, 132 Fisciano (Salerno), Italy

Corresponding Authors: Sébastien Livi (sebastien.livi@insa-lyon.fr); Giuliana Gorrasi (ggorrasi@unisa.it)

Abstract

Phosphonium ionic liquid (IL) combined with 2-ethylhexanoate counter anion has been used as interfacial agent of layered double hydroxide (LDH). First, the intercalation of hexanoate anion between the LDH layers was confirmed by thermogravimetric analysis (TGA) and X-ray diffraction (XRD). Then, this thermally stable organophilic LDH was introduced at different amount (1, 3 and 5 wt%) into pectin matrix leading to an increase of the thermal stability of the resulting nanocomposites (+35-40°C). In addition, the good distribution of the modified LDH led to an increase of the mechanical performances through the elastic moduli (+60 %) as well as a significant increase of the water barrier properties of two orders of magnitude for the pectin containing 5 wt% of LDH-IL.

Keywords: Pectins, Layered double hydroxides, Ionic liquids

1. Introduction

In recent decades the interest in obtaining new composite materials with well adapted functionalities to different technological applications is gaining more and more. Such composites, compared with the single components show improvement in mechanical, thermal, permeation, optical and chemical properties and resistance to solvents. In this context, the production of new high added value materials from sustainable, renewable and abundant sources is not only strategic from technological and economical viewpoints, but also from an environmental perspective. Such bio-based materials are an important alternative in decreasing the production of materials from non-renewable sources, solving problems caused by the emission of pollutants into the environment. Pectin are typical examples of renewable biodegradable polymeric matrices that have attracted research investments by scientific and productive sectors. They are amorphous and colloidal

35 carbohydrates of high molecular weight occurring in ripe fruits, especially in apples, currants, etc.,
36 and used in fruit jellies, pharmaceuticals and cosmetics for their thickening and emulsifying
37 properties and ability to solidify to a gel, and are classified as safe (GRAS) by the Food and Drug
38 Administration. All these properties and applications have put pectin in the market of the
39 biopolymers with great potential and possibilities for future developments (Espitia, Du, Avena-
40 Bustillos, Ferreira Soares & McHugh, 2014). The use of bio-based polymers, like pectins, has been
41 strongly limited for their inferior mechanical and barrier properties as compared to synthetic
42 polymers. For these reasons they are often blended with other synthetic polymers or, in some cases,
43 chemically modified to extend their specific applications. Hybrid organic-inorganic systems and, in
44 particular, systems in which layered silicates are dispersed at a nanometric level in a polymeric
45 matrix, are more and more emerging technologies able to overcome several drawbacks of bio-based
46 polymers. Such nanohybrids show unusual properties, very different from their microscale
47 counterparts, such as improved mechanical and oxidation stability, decreased solvent uptake, self-
48 extinguishing behavior and, in many cases, better biodegradability. The application of
49 nanocomposites will help to expand the use of edible and biodegradable films (Gorrasi, 2015;
50 Lagaron & Rubio, 2011; Mangiacapra, Gorrasi, Sorrentino & Vittoria, 2006; Ray & Bousmina,
51 2005; Makaremi et al., 2017; Biddeci et al., 2016; Cavallaro, Lazzara & Milioto, 2013). Among the
52 lamellar solids Layered Double Hydroxides (LDHs) are an interesting class of filler with flexible
53 chemistry options, good anion exchange capacity in the interlayer and good thermal stability (Rives,
54 2001). The possibility to modify these clays with a wide spectrum of organic molecules open new
55 and interesting opportunities to impart to polymeric materials novel functionalities and structural
56 performances. Recently, a new class of organic molecules has appeared as an alternative to the
57 ammonium salts commonly used as surfactant agents of layered silicates, especially
58 montmorillonite (MMT). In fact, ionic liquids (ILs) are organic salts having low melting
59 temperatures ($< 100^{\circ}\text{C}$) and are known to possess an excellent thermal stability as well as a low
60 vapor pressure. For these reasons, thermostable ionic liquids such as imidazolium or phosphonium
61 salts have been used as surfactants of clays such as montmorillonite or LDH leading to
62 improvements in the final properties but also a better distribution of clay layers in the polymeric
63 materials. In fact, the use of organically modified montmorillonites or LDHs can significantly
64 increase the thermal, mechanical and water vapor barrier properties of polymer matrices. (Livi,
65 Duchet-Rumeau & Gérard, 2011; Livi, Duchet-Rumeau & Gérard, 2014 ; Livi, Duchet-Rumeau,
66 Pham & Gérard, 2010; Livi, Duchet-Rumeau, Pham & Gérard, 2011; Livi, Dufour, Gaumont &
67 Levillain, 2013; Livi, Sar, Bugatti, Espuche & Duchet-Rumeau, 2014). Different authors such as
68 Kredatusova et al, Soares et al and Ha et al have demonstrated that ILs can be used as interfacial

69 agent of LDH. Recently, Soares et al have highlighting the intercalation of zwitterionic ionic liquid
 70 into clay layers (Moreira, De Camargo, Marconcini & Mattoso, 2013; Vartiainen et al., 2010; Saha
 71 et al., 2016; Kredatusova et al., 2016; Ha & Xanthos, 2010 e 2011; Soares, Ferreira & Livi, 2017).
 72 More recently, Kredatusova et al have used three phosphonium ILs as surfactant agents of LDH and
 73 they have highlighted that the use of ILs induced an exfoliation of the LDH sheets into
 74 polycaprolactone matrix. Other authors such as Bugatti et al have showed that improvements in
 75 water barrier properties of 30% are observed when the LDH were deposited on a PLA film
 76 previously treated by plasma treatment.

77 In this paper we report the preparation and analysis of structural and physical and barrier properties
 78 of novel composites based on natural pectins and LDH with phosphonium ionic liquid combined
 79 with 2-ethylhexanoate counter anion at different loading (i.e. 1; 3; 5 wt%). The aim was to
 80 investigate the role of interfacial agent of the ionic liquid on the morphologies as well as the final
 81 properties of natural pectins for potential food packaging applications.

82

83 2. Experimental

84

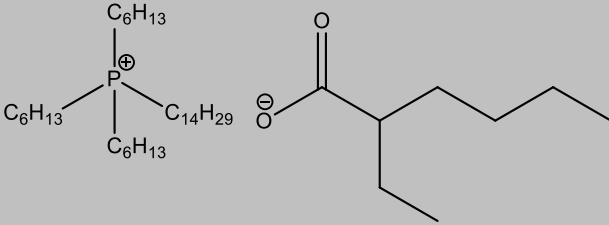
85 2.2 Materials

86

87 A layered double hydroxide (aluminum magnesium hydroxy carbonate) denoted PURAL® MG 63
 88 HT was chosen as pristine anionic clay and was provided by Sasol Performance Chemicals. The
 89 ionic liquid denoted P2 is based on (trihexyl)tetradecylphosphonium cation associated with 2-
 90 ethylhexanoate counter anion were kindly provided by Cytec Industries Inc (Canada). The ionic
 91 liquid P2 and the designation of the ionic liquid used as well as the modified LDH (LDH-P2) are
 92 summarized in Scheme 1. Pectins from apples were purchased from Sigma Aldrich in powder form.
 93 The molecular weight is 30,000-100,000 and the degree of esterification about 70-75%, on a dry
 94 basis, total impurities ≤10% water, CAS Number: 9000-69-5.

95

96 **Scheme 1.** Designation of phosphonium ionic liquid used for the surface treatment of LDH

Ionic Liquid	Chemical Structure	Designation
Trihexyl(tetradecyl)phosphonium 2-ethylhexanoate		LDH-P2

97

98

2.3 LDH-Ionic liquid preparation:

99

100 To remove the carbonate anions of the pristine LDH, a pre-treatment was required consisting to heat
101 during 24 hours at 500 °C in order to generate calcined LDH. Then, based on the anion exchange
102 capacity (AEC = 3.35 meq/g) of the layered double hydroxide used (Bugatti et al., 2013; Livi,
103 Bugatti, Estevez, Duchet-Rumeau & Giannelis, 2012; Kredatusovà et al., 2016). LDH and 2 AEC of
104 phosphonium ionic liquid combined with 2-ethylhexanoate counter anion (P2) was firstly dispersed
105 in 200 mL of deionized water/THF mixture (150/50 mL). The suspension was stirred and mixed at
106 60°C during 24 hours. The precipitate obtained was filtered and washed various times with THF.
107 The residual solvent was removed by evaporation under vacuum and finally, the treated LDH was
108 dried during one night at 80°C.

109

110

2.4 Composite films preparation

111

112 1 g of pectin and filler at different loading (i.e. 1; 3; 5 wt%) were dissolved in 25 ml of distilled
113 water at T=70°C for 1 hour. Solution of composites were then milled at room temperature in a
114 Retsch (Germany) centrifugal ball mill (model S 100), using a cylindrical steel jar of 50 cm³ with 5
115 steel balls of 10 mm of diameter. The rotation speed used was 580 rpm and the milling time was 1
116 h. Due to the short milling time, we exclude any hydrolysis phenomenon that can causes decreasing
117 of Mw of the polymer matrix. The mixtures obtained were slowly evaporated in Petri dishes. Films
118 of pure pectin were obtained in the same described experimental conditions. All films, having the
119 same thickness (\cong 150 μ m), were dried in a vacuum oven at room temperature for 5 days.

120

121

2.5 Methods of investigation

122

123 *Transmission electron microscopy (TEM)* was carried out using a Philips CM 120 field emission
124 scanning electron microscope with an accelerating voltage of 80 kV. The samples were cut using an
125 ultramicrotome equipped with a diamond knife, to obtain 60-nm-thick ultrathin sections. Then, the
126 sections were set on copper grids.

127 *X-ray diffraction (XRD)* patterns were taken, in reflection, with an automatic Bruker diffractometer
128 equipped with a continuous scan attachment and a proportional counter, using nickel-filtered Cu K α
129 radiation (K α = 1.54050 Å) and operating at 40 kV and 40 mA, step scan 0.05° of 2 Θ and 3 s of
130 counting time.

131 *Thermogravimetric analyses (TGA)* were carried out in air atmosphere with a Mettler TC-10
132 thermobalance from 30°C to 800 °C at a heating rate of 10 °C/min.

133 *Fourier transform infrared (FT-IR)* absorption spectra were recorded by a Perkin-Elmer
134 spectrometer, model Vertex 70 (average of 32 scans, at a resolution of 4 cm⁻¹). Composite films,
135 having the same thickness (\cong 150 μ m) were analyzed. The LDH-P2 filler was analysed in powder
136 form after preparing a KBr based tablet (\sim 1 mg of LDH-P2 sample and \sim 100 mg of KBr)

137 *Mechanical properties* of the samples were evaluated, in tensile mode, at room temperature and
138 ambient humidity (about 50%) using a dynamometric apparatus INSTRON 4301. Experiments were
139 conducted at room temperature on pectin and composites' films with the deformation rate of 2
140 mm/min. The specimens were 10 mm wide and \cong 250 μ m thick. The initial length of the samples
141 was 10 mm. Elastic modulus was derived from the linear part of the stress-strain curves, giving to
142 the samples a deformation of 0.1%. Data were averaged on five samples.

143 *Barrier properties* of water vapor were evaluated using conventional Mc Bain spring balance
144 system, which consists of a glass water-jacketed chamber serviced by a high vacuum line for
145 sample degassing and vapor removal. Inside the chamber, samples were suspended to a helical
146 quartz spring supplied by Ruska Industries (Houston, TX) having a spring constant of 1.52 cm/mg.
147 The temperature was controlled to 30 ± 0.1 °C by a constant temperature water bath. Samples were
148 exposed to the water vapor at fixed pressures, P, giving different water activities $a = P/P_0$, where P_0
149 is the saturation water pressure at the experimental temperature. The spring position was recorded
150 as a function of time using a cathetometer. The spring position data were converted to mass uptake
151 data using the spring constant, and the process was followed to a constant value of sorption for at
152 least 24 h. Data averaged on three samples.

153 *Surface energies* of pectin and the resulting nanocomposites were determined with the sessile drop
154 method using a Contact Angle System OCA, Dataphysics®. From contact angle measurements with
155 water and diiodomethane as test liquids, the polar and dispersive components of surface energy
156 were determined using the Owens-Wendt theory (Owens & Wendt, 1969).

157

158

159 **3. Results and discussion**

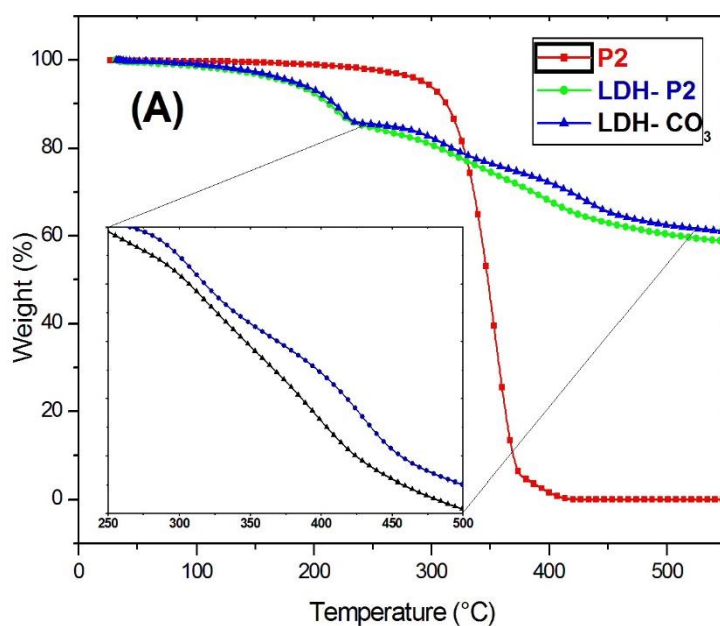
160

161 *3.1 Characterization of fillers*

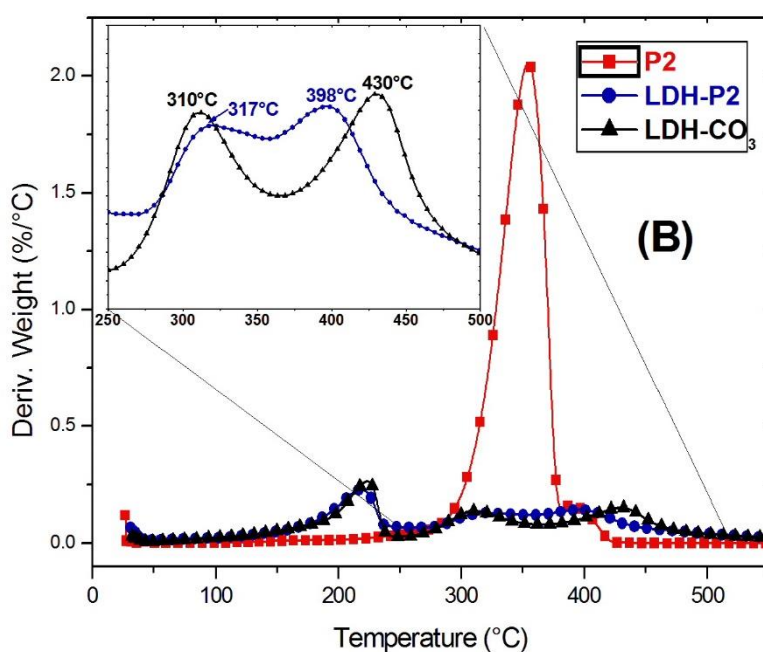
162

163 The thermal stability of P2 and LDH-P2 has been studied by thermogravimetric analysis
164 (TGA/DTG) and are shown in Figure 1 (A) and (B). In both cases, an excellent thermal stability (>

165 300°C) is observed for the phosphonium IL (P2), the pristine LDH (LDH-CO₃) and the treated-
166 LDH (LDH-P2). Indeed, a degradation temperature of around 350 ° C is observed for the ionic
167 liquid P2 while three degradation peaks are obtained for LDH-CO₃ and LDH-P2 corresponding to
168 (i) the loss of physisorbed and intercalated water molecules between LDH sheets (220 °C) and (ii)
169 the removal of interlayer carbonate anion and dehydroxylation of OH groups between 250 °C and
170 500 °C characterized in this case by two degradation peaks at 310 °C and 440 °C for LDH-CO₃, and
171 to the removal or decomposition of the physisorbed and intercalated phosphonium IL with two
172 degradation peaks at 320 °C and 396 °C for LDH-P2, respectively (Kanezaki, 1999). For LDH-P2,
173 we have attributed the first degradation peak to the presence of physisorbed ionic liquid having a
174 degradation temperature of about 340 °C whereas the second degradation peak at 396°C which is a
175 higher temperature than the intrinsic stability of P2 is assigned to the decomposition of the
176 interlayer anion. As can be seen in Figure 1 (A), the TGA curves showed a different profile between
177 250 °C and 500°C for LDH-CO₃ and LDH-P2. In fact, the presence of IL on the surface as well as
178 between the clay layers is confirmed by the formation of a large degradation peak with two different
179 degradation temperatures *i.e.* 320°C and 396°C for LDH-P2 compared to LDH-CO₃ where two
180 well-defined degradation peaks are observed at 310°C and 430°C (Figure 1 (B)). However, we can
181 also assume that a small part of the carbonate anions have been absorbed in addition to the ionic
182 liquids during the regeneration of the crystalline structure (Ha & Xanthos, 2010; Oyarzabal,
183 Mugica, Muller & Zubitur, 2016).



184



185

186

187

Figure 1: TGA (A) and DTG (B) for LDH-P2, P2 and LDH-CO₃

188

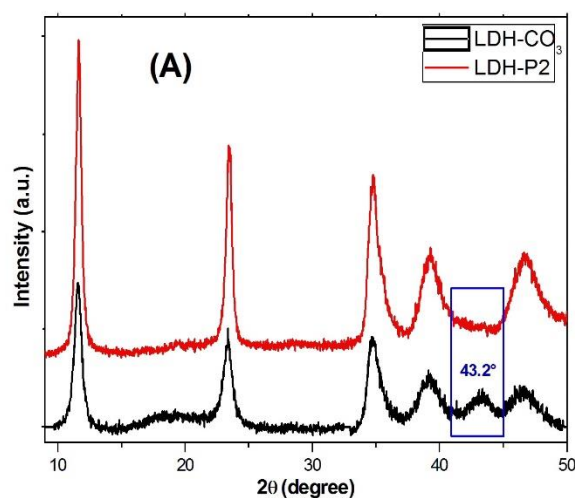
189

190

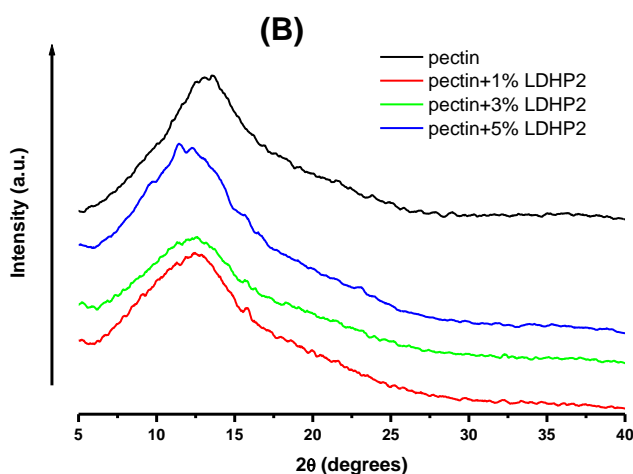
191

Figure 2 (A) reports the XRD spectra of the pristine LDH and LDH-P2. Without surface treatment, the pristine LDH and LDH-P2 showed one diffraction peak at $2\theta = 11.6^\circ$ corresponding to an interlayer distance of 7.62 \AA . In fact, no influence of the anion has been demonstrated. In summary, only the thermogravimetric analyzes presenting a different profile in function of the intercalated

192 anion confirmed the presence of the ionic liquid onto the clay surface. These assumptions have been
193 demonstrated by transmission electron microscopy (see part 3.2).



194



195

196 **Figure 2:** (A) XRD of LDH-P2 and pristine LDH-CO₃; (B) XRD of pectin and composites with LDH-P2 at
197 different loading

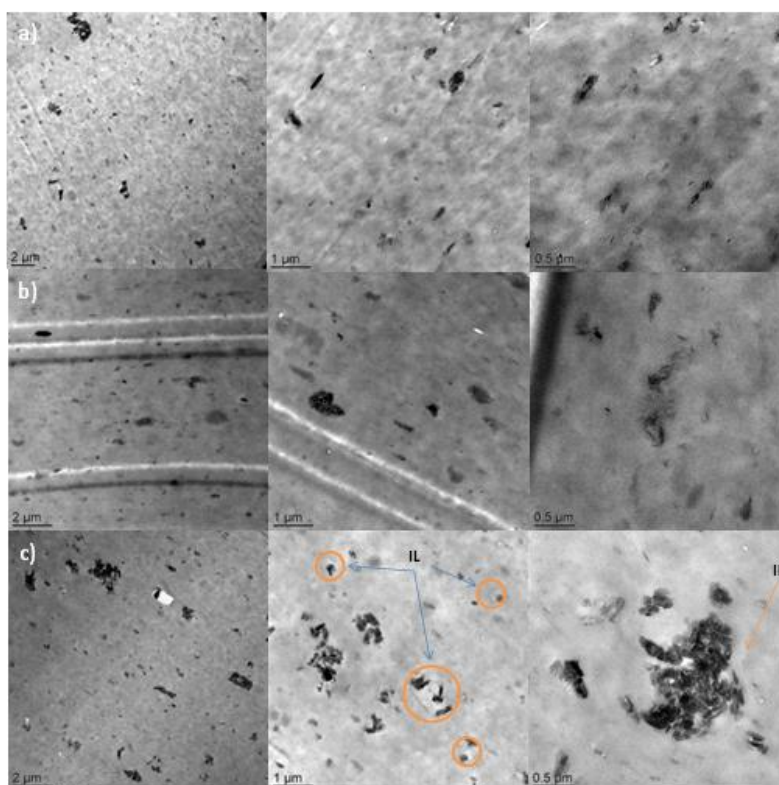
198

199 3.2 Characterization of composites

200

201 Figure 2 (B) reports the XRD of pectin and composites filled with LDH and IL. Pectin shows the
202 typical amorphous structure with one peak centered at $2\theta \approx 13^\circ$ (Gorrasi, Bugatti & Vittoria, 2012).
203 This amorphous organization is retained in all the composites. The diffraction patterns of the
204 composites do not show any other peak. This suggests that in the used milling conditions, a good
205 intercalation and/or delamination of LDH layers was reached in all cases. In order to confirm the
206 XRD results, the morphology of pectin nanocomposites containing 1, 3 and 5 wt% of organically

207 modified LDHs, transmission electron microscopy (TEM) was performed and presented in Figure 3.
208 As can be seen on TEM micrographs with two and one micrometer scale, a homogeneous and good
209 distribution of the treated LDH (LDH-P2) was observed in the pectin matrix. However, to observe
210 the morphology of the resulting nanocomposites with more precision, enlargements were performed
211 with 500 nm scale. Thus, the combined presence of some individual clay layers and few tactoids
212 having sizes of less than 1 micron were obtained, especially for pectin containing 1 and 3 wt% of
213 LDH-P2. Indeed, the formation of larger aggregates is favored by a greater amount (5 wt%) of
214 LDH-P2 (Figure 3c). In summary, the introduction of LDH-P2 into pectin induced the formation of
215 an intercalated morphology. In addition, the presence of white dots around LDH was observed on
216 the TEM micrographs of the pectin containing 5 wt% of LDH-P2 (Figure 3c). This phenomenon
217 was also revealed on the nanocomposite containing 3 wt% of LDH-P2 but not presented on this
218 paper. According to the literature, these white dots clearly highlight the presence of physisorbed IL
219 on the clay surface of LDH (Livi, 2014). In a previous paper, we have demonstrated that the use of
220 only 2 wt% of phosphonium ILs led to a phase separated morphology characterized by the
221 formation of ionic clusters into PBAT matrix (Livi, 2014). Thus, the presence of physisorbed IL on
222 the LDH surface is clearly demonstrated by TGA results as well as TEM micrographs.



223
224 **Figure 3:** TEM micrograph of a) pectin + 1%LDH-P2, b) pectin + 3%LDH-P2, c) pectin + 5%LDH-P2

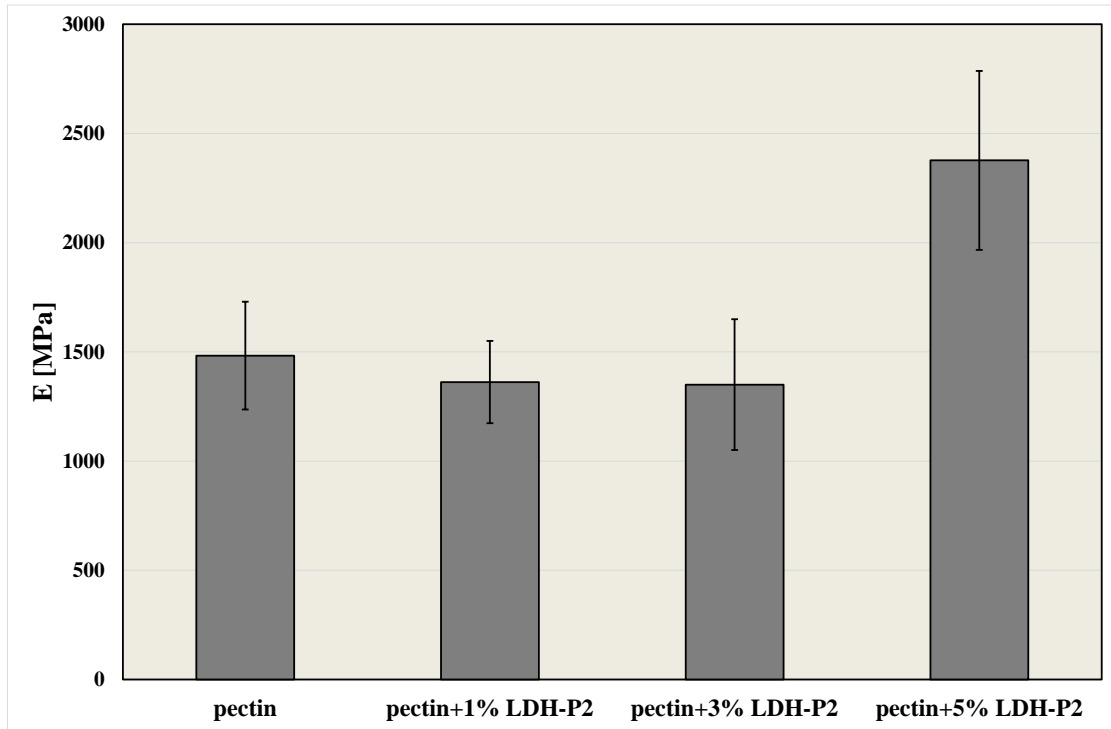
225

226 Supporting information (S1) report the FTIR spectrum, in the range 500-600 cm^{-1} , of LDH-IL,
227 pectins and composites at different filler loading, evaluated on films having the same thickness (\cong
228 150 μm) and on LDH-P2 powder mixed with KBr. It is evident that in this range pectins do not
229 show any peak, while for LDH the stretching at 553 cm^{-1} is typical of Mg-OH. In the composites
230 such peak is located at 536 cm^{-1} . This shifting suggests preferential interactions between LDH
231 sheets and -OH groups of pectin polymer matrix, being the frequency of stretching higher.

232 In supporting information (S2) it is reported the thermogravimetric analysis in air flow evaluated on
233 pure pectin and all the nanocomposites films. Pectin shows a characteristic three-step thermal
234 degradation: the first one, at about 80 $^{\circ}\text{C}$, is related to the water loss, the second, between 200 $^{\circ}\text{C}$
235 and 450 $^{\circ}\text{C}$, that covers about 50% of mass loss, is relative to primary and secondary
236 decarboxylation (Einhorn-Stoll & Kunzek, 2009). The third step between 450 $^{\circ}\text{C}$ and 700 $^{\circ}\text{C}$
237 corresponds to the oxidation region. In the nanocomposites we observe that either the second or the
238 third step delayed. The presence of the nanohybrid allows the pectin to degrade at higher
239 temperatures. It can be observed a degradation temperature at 50% of weight loss for pure pectin at
240 251 $^{\circ}\text{C}$, and at 285 $^{\circ}\text{C}$ for composite filled at 1 wt% of LDH-P2, at 288 $^{\circ}\text{C}$ for composite filled at 3
241 wt% of LDH-P2 and at 290 $^{\circ}\text{C}$ for composite filled at 5 wt% of LDH-P2. The third degradation step
242 appears much more delayed in the composites. The maximum delay can be observed for 3 wt% and
243 5 wt% of filler. Such improvement, already found for composite systems Pectin-organically
244 modified LDH (Gorrasi et al., 2012), has been attributed either to the LDH layers that create a more
245 tortuous path slowing down the diffusion of oxygen, or with a protecting effect of LDHs that
246 increases the thermal stability of the polymer matrix. It is worth noting that composites with 3% and
247 5% of LDH-P2 show a similar residue around 25%. Such residue is much higher than expected, in
248 both cases. We can hypothesize that during the thermal scan, at high temperatures (i.e. >600 $^{\circ}\text{C}$),
249 crosslinking phenomena can occur between the macromolecular chains of pectins and the IL,
250 increasing the thermal resistance of the samples. Such interesting phenomenon needs further
251 investigation.

252 Figure 4 reports the mechanical properties for unfilled pectin and composites. It was possible to
253 evaluate only the elastic moduli, E (MPa), because all samples appeared brittle and break after 0.2%
254 of deformation. Pectin itself shows a high elastic modulus, which is quite unmodified in the
255 composites filled with 1 wt% and 3 wt% of LDH-P2. The composite filled with 5 wt% of LDH-P2
256 shows an increase of the modulus of about 60% compared to unfilled sample. Considering the XRD
257 results, in which in all composites the LDH appears exfoliated, it is assumed that the extent of the
258 improvement of the modulus does not depend only upon the degree of exfoliation, but from the

259 interaction with the organic part of the filler. In this case we assume that the best interaction with
 260 the whole nano-hybrid filler is achieved at 5 wt%.



261
 262 **Figure 4:** Elastic modulus (MPa) on pectin and composites filled with LDH-P2 at different loading
 263

264 Barrier properties, sorption (S) and diffusion (D), were evaluated on all samples with the aim to
 265 analyze how the inorganic component (LDH) and the ionic liquid can affect the permeability to
 266 water vapour of pectin. Measuring the gain in weight as function of time, for the samples exposed
 267 to the vapour at a fixed partial pressure, it was possible to obtain the equilibrium value of sorbed
 268 water, C_{eq} (g solvent/100g polymer). If the transport is Fickian, that means a linear dependence of
 269 sorption versus square root of time, from the linear part of the reduced sorption curves (C_t/C_{eq} vs
 270 $t^{1/2}$) it is possible to obtain the mean diffusion coefficient using Equation (1) (Koros, Burgess &
 271 Chen, 2015):

$$\frac{C_t}{C_{eq}} = \frac{4}{d} \left(\frac{Dt}{\pi} \right)^{1/2} \quad (1)$$

272
 273 where C_t is the penetrant concentration at the time t, C_{eq} the equilibrium value, d (cm) the thickness
 274 of the sample and D (cm^2/s) the average diffusion coefficient. The sorption parameter (S) can be
 275 obtained from the equilibrium concentration (C_{eq}) of the permeant as a function of the partial
 276 pressure:

$$S = \frac{d(C_{eq})}{dp} \quad (2)$$

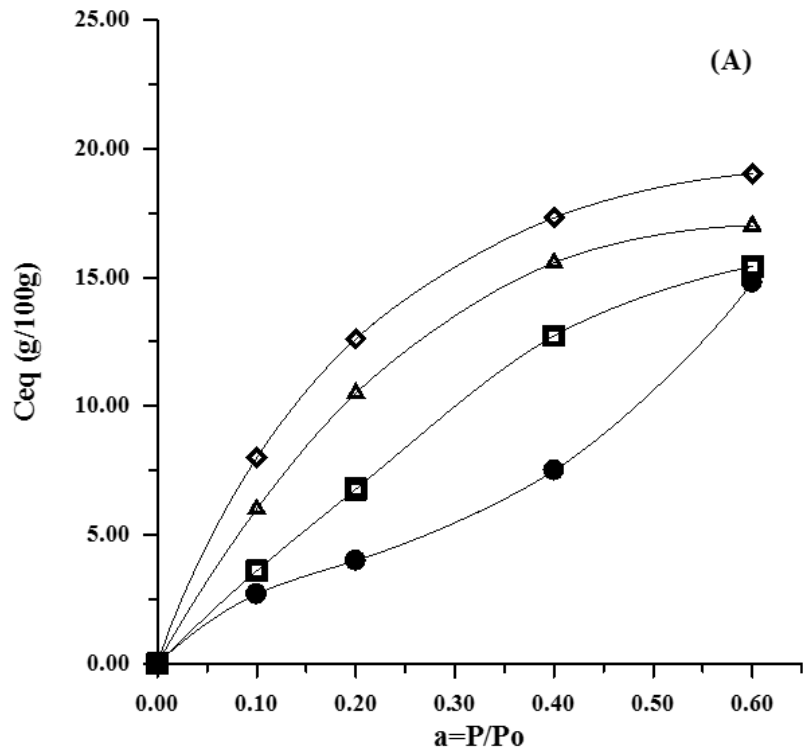
278 All considered samples showed a Fickian behavior during the sorption of water vapor at different
279 vapor activities. Using Equation (1) it was possible to derive the diffusion coefficient, D (cm^2/s), at
280 any vapor activity ($a=P/P_0$), and the equilibrium concentration of solvent into the sample,
281 $C_{eq}(\text{g}_{\text{solvent}}/100 \text{ g}_{\text{polymer}})$. For polymer-solvent systems, the diffusion parameter is dependent on the
282 vapor concentration accordingly to the empirical Equation (3):

$$283 \quad D = D_0 \exp(\gamma C_{eq}) \quad (3)$$

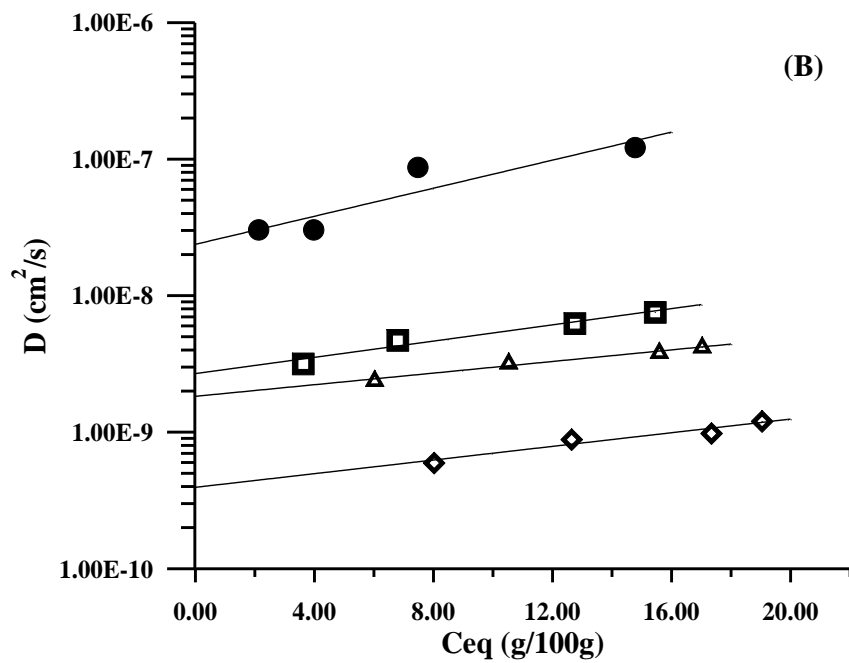
284 where D_0 (cm^2/s) is the zero concentration diffusion coefficient (related to the microstructure of the
285 polymer and to the fractional free volume), γ represents a coefficient, which depends on the
286 fractional free volume and on the effectiveness of the penetrant to plasticize the matrix (Koros,
287 Burgess & Chen, 2015). Figure 5 (A) reports the sorption isotherms as $C_{eq}(\text{g}/100\text{g})$ of sorbed water
288 as function of vapor activity, $a=P/P_0$, for all the samples. The unfilled pectin shows a dual-sorption
289 behavior. This mode is related to the fact that the besides the normal dissolution process the
290 sorption of the polar solvent occurs on preferential sites, in which the molecules are adsorbed and/or
291 immobilized. It is assumed that these specific sites on the matrix have a finite capacity and at higher
292 activities the presence of water molecules determines the plasticization of the matrix, as can be
293 observed in the transition displayed by the isotherm, as an exponential increase in vapor sorbed
294 concentration. The sorption isotherms of the composites follow a typical Langmuir mode of
295 sorption. At low activity the solvent molecules are absorbed on specific sites; when all the sites are
296 occupied a constant value of concentration is approaching on increasing the vapor pressure. The
297 increasing in the sorption is proportional with the increasing of filler loading. This is an expected
298 result, in fact it has been reported that this behavior is strictly related to the hydrophilicity of the
299 inorganic lamellae, and determines a significant dependence of water sorption on the LDH content
300 (Gorrasi et al., 2012; Gorrasi & Bugatti, 2016). The sorption parameter, S (wt\%/mmHg), was
301 evaluated in the range of activity 0-0.2, accordingly to Equation (2). Results are reported in Table 1.
302 It increased with filler loading, due to the high hydrophilicity of the filler incorporated into the
303 polymer matrix. Figure 5 (B) reports the diffusion coefficient, D (cm^2/s), as function of $C_{eq}(\text{g}/100\text{g})$
304 of sorbed water.

305
306
307
308
309
310
311

312
313
314
315



316



317

318 **Figure 5:** Sorption isotherms with respect to water vapour (A) for Pectin (●),
319 Pectin + 1% LDH-P2 (□), Pectin + 3% LDH-P2 (Δ), Pectin + 5% LDH-P2 (◇) ; diffusion coefficients as function of C_{eq} of water sorbed
320 (B) for for Pectin (●), Pectin + 1% LDH-P2 (□), Pectin + 3% LDH-P2 (Δ), Pectin + 5% LDH-P2 (◇)

321

322
323
324
325
326
327
328
329
330
331
332
333
334
335
336
337
338
339
340
341
342
343
344
345
346
347
348
349
350
351

For all samples it was extrapolated the thermodynamic diffusion coefficient, D_0 (cm^2/s), using Equation (3). Data are reported in Table 1.

Table 1. Sorption and Diffusion to water vapor

Sample	S (wt%/mmHg)	D_0 (cm^2/s) x 10^{-8}
Pectin	21.5±1.2	2.38±0.150
Pectin + 1% LDH-P2	36.2±0.7	0.270±0.0414
Pectin + 3% LDH-P2	60.1±2.3	0.183±0.0214
Pectin + 5% LDH-P2	80.2±4.2	0.0421±0.0325

The diffusion coefficients decrease with filler loading, in all the investigated composition range. It is evident a decreasing of one order of magnitude for samples filled with 1wt% and 3 wt% of filler, and two orders of magnitudes for the one filled with 5 wt%. As previously discussed, from the XRD analysis it has been evidenced that the pectin matrix, either unfilled or in the composites, shows the same amorphous structure, therefore the decrease of the values of D_0 can be attributed only to the presence of the LDH-P2 filler. The well intercalated LDH-P2 component can be able to increase the tortuosity of the pathway of this complex system and the IL fraction contributes to impart a good interfacial interaction between the two phases. Thus, the decreasing of D_0 with filler loading is related to both these effects. The extrapolated D_0 provides information related to the starting structure of the samples (i.e. fractional free volume and tortuosity of the path) strictly correlated to the morphological texture.

The contact angles and surface energy on the neat pectin and the resulting nanocomposites determined by the sessile drop method are detailed in Table 2. The measurements carried out by the sessile drop method clearly confirmed the previous results obtained for the sorption. In fact, the addition of layered double hydroxide modified by the ionic liquid denoted P2 led to a decrease in the water contact angle corresponding to an increase in the polar component with values included between 9.3 and 18.2 mN/m instead of 3.5 mN/m for the pure pectin. Thus, an increase in the hydrophilicity is observed which can be attributed to the presence of LDH and mainly to the presence of water physisorbed and intercalated onto the surface of LDH and between the clay layers.

352 **Table 2.** Polar and dispersive components of the surface energy on the neat pectin and the resulting
 353 nanocomposites, from contact angles with water and diiodomethane
 354

Sample	$\theta_{\text{water}} (^{\circ})$	$\theta_{\text{CH}_2\text{I}_2} (^{\circ})$	Surface Energy (mN/m)	Dispersive Component (mN/m)	Polar Component (mN/m)
Pectin	81,9 \pm 1	47.8 \pm 2	35.2	31.7	3.5
Pectin + 1% LDH-P2	64.5 \pm 3	37.7 \pm 2	44.1	32.4	11.6
Pectin + 3% LDH-P2	58.2 \pm 6.8	44.9 \pm 3.6	44.9	26.7	18.2
Pectin + 5% LDH-P2	65.0 \pm 5.3	37.7 \pm 3.7	42.5	33.2	9.3

355

356

357 4. Concluding remarks

358

359 In this study, new thermally stable organophilic layered double hydroxide (LDH) based on
 360 phosphonium ionic liquid (IL) surfactant has been prepared and used as filler of pectin matrix.
 361 Pectin nanocomposites with improved properties have been processed in order to investigate the
 362 role of surfactant agent of the ionic liquid on the morphologies as well as the final properties of
 363 natural pectins. The addition of different amounts of treated LDH denoted LDH-P2 led to
 364 significant improvements in the thermal stability of the pectin nanocomposites characterized by an
 365 increase of + 35- 40 ° C but also an improvement of about 60% of the mechanical performances
 366 performed in static tensile mode. Moreover, the good dispersion of treated LDH in the pectin
 367 matrix, which was investigated by transmission electron microscopy, induced significant
 368 improvement in water vapor barrier properties, in terms of decreased diffusion of two orders of
 369 magnitudes for the pectin containing 5 wt% of LDH-P2. These results open new perspectives in the
 370 field of LDH-based polymer nanocomposites and potentially in food packaging applications.

371

372 **Acknowledgements:** This work was supported by the project “High Performing Advanced Material
 373 Platform For Active and Intelligent Food Packaging: Cronogard™” (H2020-SMEINST-2-2016-
 374 2017). Grant agreement n. 783696

375

376

377

378

379

380

381

5. References

- 382
383
- 384 Biddeci, G., Cavallaro, G., Di Blasi, F., Lazzara, G., Massaro, M., Milioto, S., Parisi, F., Riela, S. &
385 Spinelli, G. (2016). Halloysite nanotubes loaded with peppermint essential oil as filler for functional
386 biopolymer film. *Carbohydrate Polymers*, 152, 548-557.
- 387
- 388 Bugatti, V., Livi, S., Hayrapeytan, S., Wang, Y., Estevez, L., Vittoria, V. & Giannelis, E.P. (2013).
389 Deposition of LDH on plasma treated polylactic acid to reduce water permeability. *Journal of*
390 *Colloid and Interface Science*, 396, 47-52.
- 391
- 392 Cavallaro, G., Lazzara, G. & Milioto, S. (2013). Sustainable nanocomposites based on halloysite
393 nanotubes and pectin/polyethylene glycol blend. *Polymer Degradation and Stability*, 98 (12), 2529-
394 2536.
- 395
- 396 Einhorn-Stoll, U. & Kunzek, H. (2009). The influence of the storage conditions heat and humidity
397 on conformation state transitions and degradation behaviour of dried pectins. *Food Hydrocolloids*,
398 23, 856-866.
- 399
- 400 Espitia, P. J. P., Du, W., Avena-Bustillos, R., Ferreira Soares, N. & McHugh, T. H. (2014). Edible
401 films from pectin: Physical-mechanical and antimicrobial properties - A review. *Food*
402 *Hydrocolloids*, 35, 287-296.
- 403
- 404 Gorrasi, G. & Bugatti, V. (2016). Edible bio-nano-hybrid coatings for food protection based on
405 pectins and LDH-salicylate: Preparation /and analysis of physical properties, LWT. *Food Science*
406 *and Technology*, 69, 139-145.
- 407
- 408 Gorrasi, G. (2015). Dispersion of halloysite loaded with natural antimicrobials intopectins:
409 Characterization and controlled release analysis. *Carbohydrate Polymers*, 127, 47-53.
- 410
- 411 Gorrasi, G., Bugatti, V. & Vittoria, V. (2012). Pectins filled with LDH-antimicrobial molecules:
412 Preparation, characterization and physical properties. *Carbohydrate Polymers*, 89, 132-37.
- 413 Ha, J. U. & Xanthos, M. (2010). Novel modifiers for layered double hydroxides and their effects on
414 the properties of polylactic acid composites. *Applied Clay Science*, 47, 303-310.
- 415

416 Ha, J. U. & Xanthos, M. (2011). Sequential modification of cationic and anionic nanoclays with
417 ionic liquids. *Green Chemistry Letters and Reviews* 4, 103.

418

419 Kanezaki, E. (1999). Intercalation of naphthalene-2,6-disulfonate between layers of Mg and Al
420 double hydroxide: preparation, powder X-Ray diffraction, fourier transform infrared spectra and X-
421 Ray photoelectron spectra. *Materials Research Bulletin*, 34 (9), 1435-1440.

422

423 Koros, W. J., Burgess, S. K. & Chen, Z. (2015). Polymer Transport Properties, *Encyclopedia of*
424 *Polymer Science and Technology*, DOI: 10.1002/0471440264.pst376.pub2.

425

426 Kredatusová, J., Beneš, H., Livi, S., Pop-Georgievski, O., Ecorchard, P., Abbrent, S., Pavlova, E. &
427 Bogdał, D. (2016). Influence of ionic liquid-modified LDH on microwave-assisted polymerization
428 of ϵ -caprolactone. *Polymer*, 100, 86-94.

429

430 Lagaròn, J. M. & Rubio, A. L. (2011). Nanotechnology for bioplastics: opportunities, challenges
431 and strategies. *Trends in Food Science & Technology*, 22, 611-617.

432

433 Livi, S., Bugatti, V., Estevez, L., Duchet-Rumeau, J. & Giannelis, E.P. (2012). Synthesis and
434 physical properties of new layered double hydroxides based on ionic liquids: Application to a
435 polylactide matrix. *Journal of Colloid and Interface Science*, 388, 123-129.

436

437 Livi, S., Duchet-Rumeau, J. & Gérard, J.F. (2014). Effect of Ionic Liquid Modified Synthetic
438 Layered Silicates on Thermal and Mechanical Properties of High Density Polyethylene
439 Nanocomposites. *Macromolecular Symposia*, 342, 46-55.

440

441 Livi, S., Duchet-Rumeau, J., Gérard, J. F. (2011) Tailoring of interfacial properties by ionic liquids
442 in a fluorinated matrix based nanocomposites. *European Polymer Journal*, 47, 1361-1369.

443 Livi, S., Duchet-Rumeau, J., Pham, T. N. & Gérard, J. F. (2010). A comparative study on different
444 ionic liquids used as surfactants: Effect on thermal and mechanical properties of high-density
445 polyethylene nanocomposites. *Journal of Colloid and Interface Science*, 349, 424-433.

446

447 Livi, S., Duchet-Rumeau, J., Pham, T. N. & Gérard, J. F. (2011). Synthesis and physical properties
448 of new surfactants based on ionic liquids: Improvement of thermal stability and mechanical

449 behaviour of high density polyethylene nanocomposites. *Journal of Colloid and Interface Science*,
450 354, 555-562.

451

452 Livi, S., Dufour, C., Gaumont, A. C. & Levillain, J. (2013). Influence of the structure of the onium
453 iodide salts on the properties of modified montmorillonite. *Journal of Applied Polymer Science*,
454 127, 4015-4026.

455

456 Livi, S., Sar, G., Bugatti, V., Espuche, E. & Duchet-Rumeau, J. (2014). Synthesis and physical
457 properties of new layered silicates based on ionic liquids : improvement of thermal stability,
458 mechanical behaviour and water permeability of PBAT nanocomposites. *RSC advances*, 4, 26452-
459 26461.

460

461 Livi, S., Bugatti, V., Soares, B.G., Duchet-Rumeau, J., (2014). Structuration of ionic liquids in a
462 poly(butylene-adipate-co-terephthalate) matrix: Influence on the water vapour permeability and
463 mechanical properties. *Green Chemistry*, 16 (8), 3758-3762.

464

465 Makaremi, M., Pasbakhsh, P., Cavallaro, G., Lazzara, G., Aw, Y. K., Lee, S. M. & Milioto, S.
466 (2017). Effect of Morphology and Size of Halloysite Nanotubes on Functional Pectin
467 Bionanocomposites for Food Packaging Applications. *ACS Appl. Mater. Interfaces*, 9 (20), 17476-
468 17488.

469

470 Mangiacapra, P., Gorrasi, G., Sorrentino, A. & Vittoria, V. (2006). Biodegradable nanocomposites
471 obtained by ball milling of pectin and montmorillonites. *Carbohydrate Polymers*, 64, 516-523.

472

473 Moreira, F. K. V., De Camargo, L. A., Marconcini, J. M. & Mattoso, L. H. C. (2013).
474 Nutraceutically Inspired Pectin–Mg(OH)₂ Nanocomposites for Bioactive Packaging Applications.
475 *Journal of Agricultural and food chemistry*, 61, 7110-7119.

476

477 Owens, D.K. & Wendt, R.C. (1969). Estimation of the surface free energy of polymers. *Journal of*
478 *Applied Polymer Science*, 13, 1741-1747.

479

480 Oyarzabal, A., Mugica, A., Muller, A. J. & Zubitur, M. (2016). Hydrolytic degradation of
481 nanocomposites based on poly(L-lactic acid) and layered double hydroxides modified with a model
482 drug. *J. Appl. Polym. Sci.*, DOI:10.1002/APP.43648.

483

484 Ray, S. S. & Bousmina, M. (2005). Biodegradable polymers and their layered silicate
485 nanocomposites: In greening the 21st century materials world. *Progress in Materials Science*, 50,
486 962-1079.

487

488 Rives, V. (2001). *Layered Double Hydroxides: present and future*. New York: Nova Science
489 Publisher Inc.

490

491 Saha, N. R., Sarkar, G., Roy, I., Rana, D., Bhattacharyya, A., Adhikari, A., Mukhopadhyay, A. &
492 Chattopadhyay, D. (2016). Studies on methylcellulose/pectin/montmorillonite nanocomposite films
493 and their application possibilities. *Carbohydrate Polymers*, 136, 1218.

494

495 Soares, B. G., Ferreira, S. C. & Livi, S. (2017). Modification of anionic and cationic clays by
496 zwitterionic imidazolium ionic liquid and their effect on the epoxy-based nanocomposites. *Applied*
497 *Clay Science* 135, 347–354.

498

499 Vartiainen, J., Tammelin, T., Pere, J., Tapper, U. & Harlin, A. (2010). Biohybrid Barrier Films from
500 Fluidized Pectin and Nanoclay. *Carbohydrate Polymers*, 82, 989-996.